Scalable 4-D Printed Tactile Sensor For The Detection Of Shear Forces In Aid Of Plantar Measurements

Constantinos Heracleous[1,2], Julian JH Leong[1,3], Rui CV Loureiro[1,2,3]
[1] Aspire Centre for Rehabilitation Engineering and Assistive Technology, University College London, HA7 4LP, UK
[2] Wellcome/EPSRC Centre for Interventional and Surgical Science, University College London, London, WC1E 6BT, UK
[3] Royal National Orthopaedic Hospital, Brockley Hill, Stanmore HA7 4LP, UK
Constantinos.Heracleous.18@ucl.ac.uk

***Abstract*—A variety of sensing technologies have been proposed to measure loading on the plantar surface of the human foot. The majority have a single measurement axis, and few are designed with multiple measurement axes capable of monitoring normal and shear stress. This paper proposes a low cost, biocompatible triaxial piezoresistive sensor that can be implemented with a simple fabrication using inexpensive equipment. The sensor can detect pressures from 0-800kPa with high response and recovery with minimum hysteresis and repeatable results for more than 100 cycles.**

Keywords— FDM 4D printing, force-sensitive sensor, flexible sensors, plantar force measurements

I. Introduction

State of the art tactile sensors are primarily based on inorganic silicon [1], [2], organic semiconductors [3][4][5], carbon nanotubes [6], graphene nanoplatelets [7], pressure-sensitive rubber [8], self-powered devices [9][10] are susceptible and can be applied to human skin. However, they have complex and expensive fabrication processes which require high-end workshops.

Various shear force sensitive sensors have been demonstrated. For example, Chase and Luo [11] developed a shear and normal force sensor with four squared electrodes at the bottom and a single squared electrode at the top of the sensor. The mechanism was based on the deflection and compression of the filler layer between the top and bottom electrodes. The shear force and direction were calculated using the ratios of the four single capacities. The drawback of this configuration is that one only obtains a tiny delta in the capacitance, especially when measuring shear force.

Lei et al. [12] developed a capacitive pressure sensor for measuring plantar load. The sensor consists of a raised 'bump' layer, a top electrode, a PDMS dielectric layer, and a bottom layer with four electrodes. This forms four independent capacitive sensing switches, which are averaged to enable robust pressure measurement up to 945 kPa, even in loads causing non-uniform deformation to the dielectric layer. In general, these sensors embed four capacitive elements, which can be used to obtain normal and shear forces through selective decoupling of the output signals. Using this approach, in 2013, Dobrzynska and Gijs [13] developed a flexible triaxial force sensor with "E"-shaped design for both the top and the bottom electrode and consists of four parallel-plate capacitors, employing a silicone dielectric. This sensor can measure load in each axis up to 14 N (equivalent to 220 kPa), offering an appropriate range for plantar shear stress measurement.

Overall, these models highlight a particular challenge in measuring shear forces. Electrode configuration and substrate integrity should be arranged to detect shear forces independently. The substrate material refers to the material that contributes to the composite flexibility rather than the charge carrier [14]. The design principle focuses on the integrity of the substrate material, where it is reformed to be able to detect normal and shear forces.

II. Sensor design

The design of the proposed structure of a three-axis tactile cell is illustrated in Fig. 1a. It consists of five different layers. The structure and materials shown as b, i, e_{top}, s, p, and e_{bot} indicate the thickness of the negative bump (silicone elastomer Mold Max™ 10), an insulation layer (Kapton tape), top electrode (copper tape), 3d printed semiconductive substrate (Ninjatek eel), PDMS (SYLGARD 184) spacer, and bottom copper electrode, respectively. The size of the cell is 10×10mm. In each sensor cell, there are four resistors located on each corner of the substrate to form a 2×2 array. The negative bump has four positive bumps at each corner of the cell and is situated in the centre above the upper electrode insulation layer. The PDMS spacer is located between the bottom electrode and substrate. Four gaps are formed from the design of the substrate, as shown in Fig. 1c. The gap distance, dz, on each resistor is determined by the direction of the applied force. The mechanism works like a seesaw where torque is generated at the pivot points shown in Fig. 1b Two see-saw mechanisms are formed and responds to the direction of the shear force when the moments on each side are uneven. Consequently, when a normal force is applied to the top of the cell, the substrate is compressed, and the four air gaps between the electrodes decrease identically. This behaviour implies an equivalent resistance change for the four resistors. On the other hand, when a normal and shear force is applied to one direction, the substrate produces a torque, incrementing the gaps for one resistor towards the applied shear force direction as shown in Fig.1d. As a result, based on the resistance variation, the applied normal and shear force can be sensed differently.

The work is funded by Biederman Motech GmbH Co and partially supported by the Wellcome Trust and EPSRC through the WEISS Centre (grant: 203145Z/16/Z) at UCL.

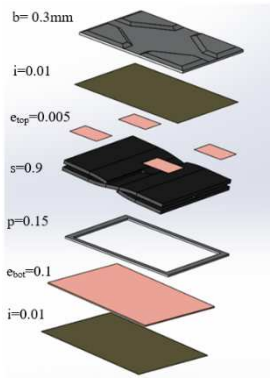

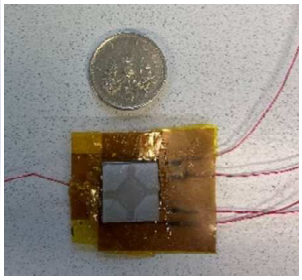

Fig. 1b sensor screenshot

Fig. 1a sensor layers and materials

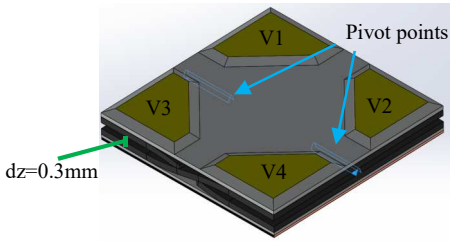

Fig. 1c Sensor composite structure annotating in yellow V1, V2, V3, V4 of each resistor, pivot points in blue and dz gap disctance between the two substrates.

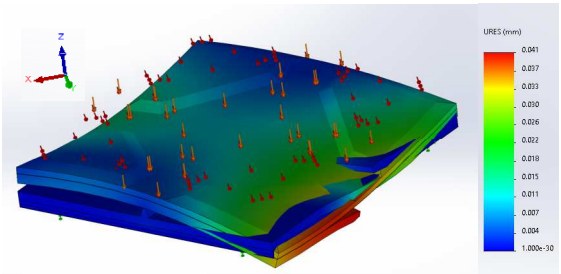

Fig. 1d Deformed part from normal and shear pressure

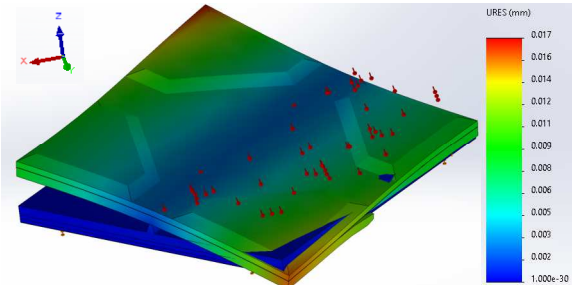

Fig. 1f Deformed part from shear pressure

Finite Element Analysis was performed in Solidworks using a 3D model to verify the mechanical principle. Material properties were used from datasheets from all materials forming the tactile cell [15],[16],[17]. An elastic model for analysis was employed since the stress-strain curve of the materials used is almost linear, and the hysteresis is negligible for small deformations. Normal (z) and shear force (y) were applied across the whole top surface of the cell as illustrated in Fig. 1d. The boundary condition for the bottom of the model has been fixed in all directions. The figure's colour gradient displays the calculated displacement in z-direction under shear pressures where blue indicates minimum displacement regions and red the maximum ones. As shown in Fig. 1f, the cell deforms as expected for shear pressures applied on the x and y-axis.

III. Electrical Model

The sensor was modelled with a simple approach using four resistors in parallel located at the corners of the sensor. The four resistors in Eq. (1) are four independent sensing elements for normal and shear loads detection.

$$\frac{1}{R1}+\frac{1}{R2}+\frac{1}{R3}+\frac{1}{R4}=Re \tag{1}$$

It is assumed that there is no influence on the wiring since the length of each wire was equal for each connection. Negligible strain is present on the x and y components since the load applied to the sensor is compression and not tension. Therefore, the z component maximum strain is present. The areas of all four-square electrodes were designed identically with the area A = A1 = A2 = A3 = A4. The theoretical model assumes that the resistivity is equally thick across the entire sensor with a thickness of d. Therefore, the resistivity Eq. (2) can be employed for the initial resistance Re:

$$Re=\frac{\rho L}{A} \tag{2}$$

A force in the z-direction reduces the distance by Δdz, decreasing all four resistors' resistance there Rz is the sum of all resistors as in Eq. (3). A force in the x-direction increases the thickness of the resistor R1 by Δdx and decreases the thickness of R3 to the same extent while not influencing R2 and R4. A subtraction of each pair of resistance indicates the applied shear forces in the x- and y-direction, as shown in Eq. (4)(5).

$$Rz=R1+R2+R3+R4=\frac{dt_{R1}+dt_{R2}+dt_{R3}+dt_{R4}}{t} \tag{3}$$

$$Rx=R1-R3=\frac{dt_{R1}-dt_{R3}}{t} \tag{4}$$

$$Ry=R2-R4=\frac{dt_{R2}-dt_{R4}}{t} \tag{5}$$

IV. Fabrication Process

The sensor consists of the two identical semiconductive flat substrates packaged. The design was performed in Solidworks and the material used was a carbon black fused filament. Ninjatek Eel is a flexible conductive filament, that carbon black. Surface treatments such as wet etching were used to form electrodes. Firstly, copper tape and the Kapton tape were adhered together avoiding any air vents between the two surfaces as shown in Fig. 2a. A photosensitive film was used as a mask to form the desired electrode location with its connection traces. Photolithography then penetrated the film leaving the negative profile of electrode configuration Fig.2b, c. The etching process follows by using a positive developer (NaOH) to remove the penetrated traces of the mask Fig.2d. Finally, the PI-Cu laminate was exposed to FeCl acid to complete etching Fig.6e. This results in a 5.5

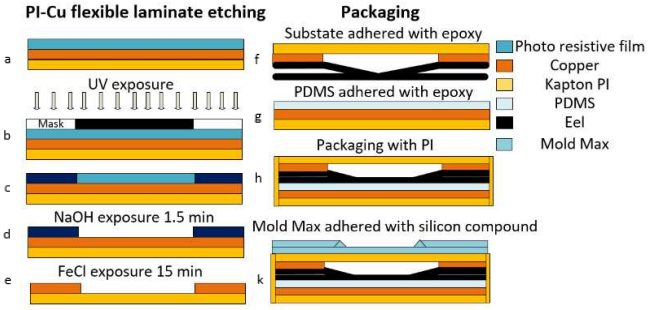

Fig. 2 Fabrication process; surface treatments and packaging

µm thick copper electrode with 6.3µm of insulation. Finally, wires are soldered to the copper pads in the PI-Cu laminate. PDMS spacer was formed by mixing the two parts and degassing them. To form a thin layer for the spacer the uncured silicone was poured on a flat surface and agitated using an orbital shaker. Then placed in a convection oven at 80 $°C$ for approximately 1 hour 30 minutes until the PDMS was completely dry. Finally, cut into shape using square-shaped

hole punchers. Silicone MoldMax 10T was used to create the top encapsulated layer using the moulding method to achieve the desired profile. Packaging was done manually by stacking part g and f with the encapsulation on top, as shown in Figure 2f-k.

V. Experimental Results and Discussion

Sensor performance was characterized using a uniaxial Mechanical test machine (Zwigg Roel). A rigid indentor covering the whole surface of the cell was used to apply a known load. The cell was attached to a silicone slab to mimic the natural environment mechanics of plantar forces because the applied force from the foot is striking the shoe elastomer and not the ground. 5V, 0,3A DC power supply to the bottom electrode of the sensor and TEKTRONIX 4 channel oscilloscope were used to measure the voltage change on the top electrodes through a voltage divider circuit. Firstly, to find hysteresis, response recovery, repeatability, and fatigue resistance of voltage change, a cyclic fatigue test was used, applying a constant load of 10N with 300ms hold for 100 cycles. Secondly, a creep test was prompted to find relaxation by holding a constant load of 20N for 1 hour. Thirdly, to find the sensitivity of the tactile cell, a stepwise load test was conducted ranging from 1 to 80N, with an increment of 1N per step. Lastly, zero drift time was found by supplying a constant current for 1 hour.

Table 1 summarizes the overall performance of the sensor cell. Figures 3b and c show the raw data from the cyclic fatigue test and creep load. Results show that after ten cycles, repeatability lies within 4%. The creep test showed that the sensor relaxation has a deviation of 5% within 30 minutes of holding a constant load. Hysteresis is improved by the PDMS spacer enabling the sensor to return to an open circuit when not in load. Figure 3a illustrates the sensitivity of the sensor from the stepwise load test. The sensor appears linear in two regions, one between 0-200kPa with ~100 Pa/mV and another from 200 to 800kPa with 375 Pa/mV. Consequently, the cell is almost four times more sensitive to low pressures than to higher pressures. The force range could be customized upon the task.

Additionally, shear tests were performed to apply force in four directions using a triaxial controlled end effector. Initially, the force was applied normal to the cell's surface, followed by shear force on the x and y-axis from one corner to the other of the cell. Figure 4a depicts the voltage changes of the four sensing elements under x-axis shear loads where only V1 and V2 are active according to the direction of the force. Similarly, the x-axis shear testing results in Fig. 4b show that the measured voltage changes of V3 and V4 have significant signal variations compared with V1 and V2. As stated in section three z axis load is derived by the sum of all

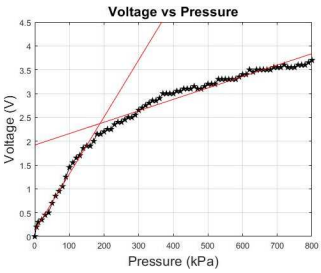

Fig. 3a Sensor sensitivity

Table 1 Sensor characteristics

Performance	Specifications
Hysteresis	2%
Response	100ms
Recovery	150ms
Repeatability	4%
Fatigue resistance	100 cycles
Relaxation	5% / 30min
Zero drift time	0.5% / h

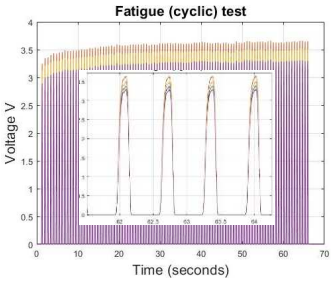

Fig. 3b Cyclic test raw data

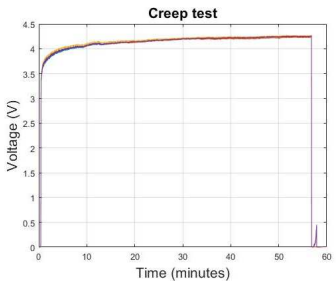

Fig. 3c Creep test raw data

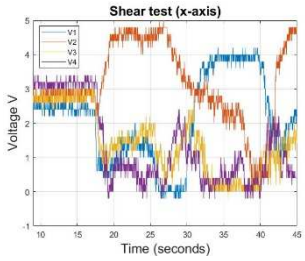

Fig. 4a Force in x axis

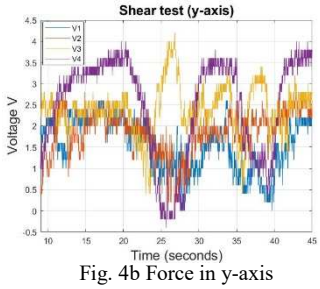

Fig. 4b Force in y-axis

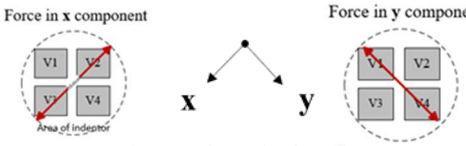

Fig. 4c Indentor load motion

voltage values. Hence, normal and shear loads can be distinguished through the proposed sensor.

VI. Conclusion

This paper describes the design and development of a low-profile planar sensor that can be used to measure shear and normal load (pressure). An array of the sensors might be configured in an instrumented insole to measure ground reaction force and the foot's centre of pressure. While the sensor was designed primarily for in-shoe application, it could also help measure shear forces between any adjacent surfaces where a small, low-profile sensor is needed. Adjustments could be made to fit the requirements of different applications. Such fine-tuning could be achieved by altering the percentage infill of 3D printing of the substrate materials or its thickness. Overall, the sensor cell shows promising results, although part to part fabrication reproducibility must be improved by changing the packaging method, which will be achieved in future work.

Acknowledgment

The authors thank the Institute of Orthopedic and MSK science technical team at UCL for their support and Dr Steve Taylor and Sara Ghoreishizadeh for their contributions.

REFERENCES

[1] Kim, D. H., Lu, N., Huang, Y., & Rogers, J. A., "Materials for stretchable electronics in bioinspired and biointegrated devices." MRS Bulletin, 37(3), 2012.

[2] Takei, K., Takahashi, T., Ho, J. C., Ko, H., Gillies, A. G., Leu, P. W., Fearing, R. S., & Javey, A., "Nanowire active-matrix circuitry for low-voltage macroscale artificial skin." Nature Materials, 9(10), 2010.

[3] Kaltenbrunner, M., Sekitani, T., Reeder, J., Yokota, T., Kuribara, K., Tokuhara, T., Drack, M., Schwödiauer, R., Graz, I., Bauer-Gogonea, S., Bauer, S., & Someya, T., "An ultra-lightweight design for imperceptible plastic electronics". Nature, 499(7459), 2013.

[4] Chortos, A., Lim, J., To, J. W. F., Vosgueritchian, M., Dusseault, T. J., Kim, T. H., Hwang, S., & Bao, Z., "Highly stretchable transistors using a microcracked organic semiconductor." Advanced Materials, 26(25), 2014.

[5] Someya, T., Sekitani, T., Iba, S., Kato, Y., Kawaguchi, H., & Sakurai, T., "A large-area, flexible pressure sensor matrix with organic field-effect transistors for artificial skin applications." Proceedings of the National Academy of Sciences of the United States of America, 101(27), 2004.

[6] Yamada, T., Hayamizu, Y., Yamamoto, Y., Yomogida, Y., Izadi-Najafabadi, A., Futaba, D. N., & Hata, K., "A stretchable carbon nanotube strain sensor for human-motion detection." Nature Nanotechnology, 6(5), 2011.

[7] Li, X., Zhang, R., Yu, W., Wang, K., Wei, J., Wu, D., Cao, A., Li, Z., Cheng, Y., Zheng, Q., Ruoff, R. S., & Zhu, H., "Stretchable and highly sensitive graphene-on-polymer strain sensors." Scientific Reports, 2, 2012.

[8] Mannsfeld, S. C. B., Tee, B. C. K., Stoltenberg, R. M., Chen, C. V. H. H., Barman, S., Muir, B. V. O., Sokolov, A. N., Reese, C., & Bao, Z., "Highly sensitive flexible pressure sensors with microstructured rubber dielectric layers." Nature Materials, 9(10), 2010.

[9] Wu, W., Wen, X., & Wang, Z. L., "Taxel-addressable matrix of vertical-nanowire piezotronic transistors for active and adaptive tactile imaging." Science, 340(6135), 2013.

[10] Wang, Z. L., "Self-powered nanosensors and nanosystems." Advanced Materials, 24(2), 2012.

[11] T. A. T. A. Chase and R. C. R. C. Luo, "A thin-film flexible capacitive tactile normal/shear force array sensor," in Proceedings of IECON '95-21st Annual Conference on IEEE Industrial Electronics, pp. 1196–1201, Orlando, FL, USA, 1995.

[12] Lei, K. F., Lee, K. F., & Lee, M. Y., "Development of a flexible PDMS capacitive pressure sensor for plantar pressure measurement. Microelectronic Engineering, 99, 2012.

[13] Dobrzynska, J. A., & Gijs, M. A. M., "Polymer-based flexible capacitive sensor for three-axial force measurements." Journal of Micromechanics and Microengineering, 23, 2013.

[14] Ninjatek eel 3d printer filament "Technical data sheet: https://ninjatek.com/wp-content/uploads/Eel-TDS.pdf"

[15] SYLGARD™ 184 Silicone Elastomer "Technical data sheet: https://www.dow.com/content/dam/dcc/documents/en-us/productdatasheet/11/11-31/11-3184-sylgard-184-elastomer.pdf?iframe=true"

[16] Silicone elastomer Mold Max™ 10 "Technical data sheet: https://www.smooth-on.com/msds/files/823A-231B.pdf"